sustainability

MDPI

Article

Safety Evaluation of Plain Concrete Lining Considering Deterioration and Aerodynamic Effects

Feng Lu [1,2,3], Yi Wang [1,*], Junfu Fu [4,*], Yanxing Yang [5], Wenge Qiu [2], Yawen Jing [2], Manlin Jiang [2] and Huayun Li [4]

[1] School of Emergency Management, Xihua University, Chengdu 610039, China; fenglu0901@foxmail.com
[2] Key Laboratory of Transportation Tunnel Engineering, Ministry of Education, School of Civil Engineering, Southwest Jiaotong University, Chengdu 610031, China
[3] Jinhua Xinsheng Zeolite Development Co., Ltd., Jinhua 321000, China
[4] School of Architecture and Civil Engineering, Xihua University, Chengdu 610039, China
[5] School of Civil Engineering, Sichuan University of Science & Engineering, Zigong 643000, China
* Correspondence: wangyi7@stu.xhu.edu.cn (Y.W.); fujunfu@stu.xhu.edu.cn (J.F.)

Abstract: With an increase in the service time of high-speed railway tunnels, various defects caused by construction-quality defects in the secondary lining begin to appear. How to evaluate the safety of such tunnels and take countermeasures is very important for the safe operation of tunnels. Based on the load-structure method and a numerical simulation, this paper studied the short-term and long-term safety of the missing section of anti-crack reinforcement mesh in the plain concrete lining of a high-speed railway mountain tunnel. The short-term safety evaluation considered the influence of negative pressure caused by aerodynamic effects. The long-term safety evaluation considered the combined influence of the surrounding rock and concrete deterioration and the negative pressure and concrete fatigue damage caused by aerodynamic effects. The results showed that under the negative pressure generated by aerodynamic effects, the minimum tensile safety factor of the lining in the defective section increased by 3.8%, while the minimum compressive safety factor of the lining decreased by 7.9%. The negative pressure generated by the aerodynamic effects had little impact on the short-term safety of the lining in the defective section. During the long-term safety evaluation, the overall safety of the defective section decreased significantly, and the minimum tensile and minimum compressive safety factors of the lining decreased by 59.4% and 66.8%, respectively. The calculation results for the initial design do not meet the long-term design requirements and cannot guarantee the long-term safe operation of the tunnel. Finally, two new strengthening methods of galvanized steel mesh-short bolts and galvanized corrugated steel plate-short bolts were proposed to strengthen the defective section of the concrete lining, so as to improve the ultimate bearing capacity and toughness of the plain concrete lining structure.

Keywords: high-speed railway tunnel; lining defects; aerodynamic effects; deterioration; safety factor; treatment measures

Citation: Lu, F.; Wang, Y.; Fu, J.; Yang, Y.; Qiu, W.; Jing, Y.; Jiang, M.; Li, H. Safety Evaluation of Plain Concrete Lining Considering Deterioration and Aerodynamic Effects. *Sustainability* **2023**, *15*, 7170. https://doi.org/10.3390/su15097170

Academic Editors: Zhixiang Yu, Yang Li, Hu Xu and Chang Yang

Received: 20 March 2023
Revised: 15 April 2023
Accepted: 24 April 2023
Published: 25 April 2023

1. Introduction

With the rapid economic development of China, more high-speed railways are under construction. As an integral part of high-speed railways, the construction scale of tunnels also increases year after year [1–3]. With the increase in the operation time of high-speed railway tunnels, many factors, such as lining structure damage [4], dry–wet cycle [5], special surrounding rock [6], frost heaving cycle [7], groundwater [8] and other factors may lead to safety risks, of which damage to the lining structure is one of the most important [9].

The deterioration of the working performance of the lining structure is mainly caused by the deterioration of the surrounding rock and concrete and construction-quality defects [10]. Especially for plain concrete lining structures, due to the lack of reinforcement, when the stress on the lining is increased due to the deterioration of the surrounding rock or when there are initial defects in the lining (such as construction cold joints [11]), the lining structure is prone to falling (Figure 1a), cracking (Figure 1b) or other defects [12], which seriously endangers operation safety. In addition, in high-speed railway tunnels, aerodynamic effects on the safety of lining structure caused by trains running cannot be ignored. For example, in 1999, the secondary lining of Fukuoka Tunnel in Japan fell off locally. The investigation results showed that long-term aerodynamic effects are one of the most important reasons for the continuous expansion of lining cracks [13]. In order to ensure the safe operation of high-speed railway tunnels for their the design life, the study of the reduction of tunnel safety due to the deterioration of the surrounding rock and concrete, lining quality defects and aerodynamic effects [14–16] has become an important topic in the traffic field.

Figure 1. Damage to the concrete lining of operational tunnels. (**a**) Collapse and (**b**) cracking.

During the long-term operation of a tunnel, due to the joint effect of internal and external factors, the surrounding rock and concrete will deteriorate, which will reduce the safety of the lining structure [10]. Sandrone et al. [17] proposed a long-term safety analysis method for tunnels based on the converging-constraint method for the deterioration of surrounding rock and concrete under aging, weathering and other conditions. Fu et al. [6] studied the gypsum rock surrounding Wuzhishan Tunnel and found that the volume of the rock increased after absorbing water, which then produced a swelling effect on the lining structure. Xu et al. [18] studied the deterioration of concrete in a freeze–thaw environment based on a numerical simulation. The results showed that with an increase in the number of freeze–thaw cycles, the deterioration of the concrete was intensified, which could cause serious cracking of the lining structure, and even collapse. Kong et al. [19] found that the deterioration of surrounding rock and concrete increased the displacement of and pressure on the second lining. Therefore, the impact of the surrounding rock and concrete deterioration should be taken into account when evaluating the safety of operating tunnels, especially when evaluating their long-term safety.

Due to the comprehensive influence of design concepts, construction conditions, geographical environment and other factors, defects in lining structures occur from time to time in the early stages of construction, which means tunnel operation may suffer potential safety hazards [20]. Ye et al. [21] found that problems such as cavities and uneven lining thickness caused by blasting were ignored during the construction of Liupanshan Tunnel, resulting in cracks, water leakage and bottom damage to the lining structure during its operation. In view of the above defects, reinforced concrete umbrella arch reinforcement measures were proposed. After a numerical analysis, the overall safety of the tunnel met the operation requirements. Lu et al. [22] put forward a reinforcement scheme of applying three-level lining in view of the insufficient thickness of the tunnel lining. The results show that after applying a three-level lining, the axial force of the initial support and the bending moment of the secondary lining were significantly reduced. Fu et al. [23] studied the defects of a monorail tunnel and found that the quality of the sprayed concrete was not strictly controlled during construction, resulting in a defect of insufficient lining thickness. Their numerical simulation study showed that the construction defects would lead to the deformation of the lining structure and to stress concentration at the defects. In addition, tunnels with arch-crown construction defects are more dangerous than tunnels with arch-shoulder construction defects. Han et al. [24] studied the stress state of tunnel structures under the conditions of a lining defect and rear cavity comprehensive defects through a numerical simulation. The results showed that the lining in the defective area was bent outward and that there was a tensile stress concentration on the outer surface and a compressive stress concentration at the edge. Yuan et al. [25] proposed a model that can predict the structural life and safety based on the concrete spalling of a tunnel's lining. Lai et al. [26] found more than 100 cracks in the lining structure of the Shitigou Tunnel due to lining defects found through an inspection. After an evaluation, it was determined that the structural damage could endanger the safety of pedestrians and vehicles, and corresponding reinforcement measures were to be taken. Gao et al. [27] conducted a study on the phenomenon of water seepage during the operation of Kaiyuansi Tunnel, and the results showed that the lining cracks, due to the failure to use the specified materials during the construction of the lining structure and the failure to strictly control the construction quality, formed a penetrating seepage channel inside.

A high-speed train passing through a tunnel will produce aerodynamic effects and bring an additional load to the lining structure. In addition, under the long-term cyclic action of the aerodynamic effects, fatigue damage to the concrete will occur, which will affect the safety of the lining structure [28]. Wang et al. [29] found that under the cyclic dynamic load of a high-speed train, micro-cracks in the concrete will further expand. If there are joints in the tunnel's concrete structure, the fatigue life of the support structure is only 56 years. When underground water remains at the tunnel site, the fatigue life will be reduced by about 20%. On the basis of a numerical simulation, Du et al. [30] proposed a double fatigue damage accumulation model for the second lining structure of high-speed railway tunnels, and its reliability was verified by indoor tests. Through this model, the influence of the aerodynamic effects of train operation on the secondary lining was analyzed. The results showed that the damage to the lining structure caused by the train running inside the tunnel was close to that caused by the train leaving the tunnel exit; the damage accumulation was proportional to the number of running trains. Li et al. [31] proposed that if a high-speed train passes through one of two closely adjacent tunnels, the aerodynamic effects generated will affect the other tunnel and the aerodynamic performance should be improved.

At present, the research on the safety evaluation of high-speed railway-tunnel lining defects mainly focuses on the impact of single factors, such as the deterioration of the surrounding rock and lining, the additional load caused by aerodynamic effects and the fatigue damage to concrete caused by aerodynamic effects. However, during the long-term service of high-speed railway tunnels, the tunnel structure is usually subject to the combined effects of lining defects, material deterioration, aerodynamic effects and concrete fatigue effects. In particular, little attention has been paid to the safety evaluation of a plain concrete lining with construction-quality defects. In view of this, this paper takes a high-speed railway mountain tunnel with a lack of anti-crack reinforcement mesh in the plain concrete secondary lining as a case study. It proposes a safety evaluation method in the case of defects in the plain concrete lining of a high-speed railway tunnel and gives treatment measures. First, the geological situation and the lack of a secondary lining reinforcement mesh are explored. Second, based on the load-structure method, the short-term safety of the lining structure under the aerodynamic effects is analyzed using a numerical simulation. The long-term safety of the lining structure is studied considering three factors, namely, the deterioration of the surrounding rock and concrete, the negative pressure load generated under the aerodynamic effects and the fatigue damage to the concrete caused by the aerodynamic effects. Finally, according to the results of short- and long-term safety analyses, improvement measures are proposed to ensure the safe operation of a tunnel within the design period. The research results can provide a reference for the safety evaluation and regulation research of concrete-lined tunnels.

2. Tunnel Overview

2.1. Geology Conditions and Lining Structure

The tunnel in this study is located in the eastern Taitou District of Zhangzhou City. The tunnel is a double-track railway tunnel with a design speed of 350 km/h. The total length of the tunnel is 1154.015 m, with a starting mileage of DK264+397.985 and an ending mileage of DK265+552. The tunnel site area is a hilly area and the maximum buried depth of the tunnel is about 92 m. The tunnel site is mainly exposed to diorite, which is distributed from completely weathered to moderately weathered. The surface water in the tunnel site area is mainly composed of atmospheric precipitation and new reservoirs at about 350 low-lying places southeast of downstream DK264+750. The groundwater is composed of bedrock fissure water and tectonic fissure water, in which bedrock fissure water is distributed in bedrock fissures and the water volume is generally poor. The structural fissure water is distributed in the fault zone of the tunnel site area, with good local water conductivity and rich groundwater. The tunnel location and geological profile are shown in Figure 2. The secondary lining of the whole tunnel is a plain concrete lined structure. In order to ensure the safety of the plain concrete lining during its service life, when the mileage of the secondary lining is within 150 m from the tunnel portal or the place where the catenary embedded channel is set, the secondary lining adopts three-leg lattice girders and a single-layer anti-crack reinforcement mesh for a strengthening treatment. The diameter of the main reinforcement of the three-leg lattice girders is 22 mm and the longitudinal spacing along the tunnel is 2 m. A single-layer reinforcement mesh is located inside the village masonry with a diameter of 16 mm and spacing of 200 × 200 mm.

2.2. Overview of Defective Section

2.2.1. Defect Description

Geological radar was used to conduct nondestructive testing on the secondary lining structure of the tunnel. According to the results (shown in Figure 3), it was found that there was a defect in the anti-crack reinforcement mesh of the tunnel's DK265+402-DK265+420 and DK265+432-DK265+456 sections. The three-leg lattice girders of the secondary lining were constructed according to the design requirements. Considering that the construction spacing of the three-leg lattice girders of the secondary lining is 2 m, and the lining between the lattice girders of the defective section is plain concrete, there is a risk of falling blocks during the service period.

According to the Code for Design of Railway Tunnels (TB 10003-2016) [32], the surrounding rock of sections DK265+402-420 and DK265+432-450 is classified as Class III, the lining support type is III_a, the secondary lining thickness is 40 cm and C30 concrete is used. The surrounding rock of section DK265+450-456 is classified as Class IV, the lining support type is IV_a, the lining thickness is 40 cm for the arch wall and 50 cm for the inverted arch and C35 concrete is used. The cross-section design of the studied tunnel at its defective section is shown in Figure 4.

(a)

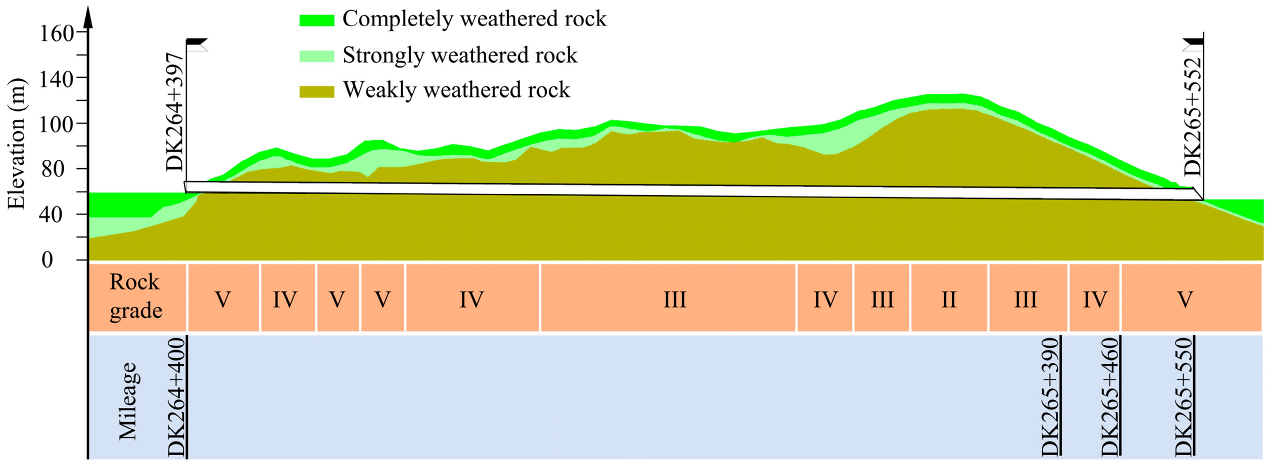

(b)

Figure 2. Tunnel location and geological profile. (**a**) Tunnel location and (**b**) geological profile.

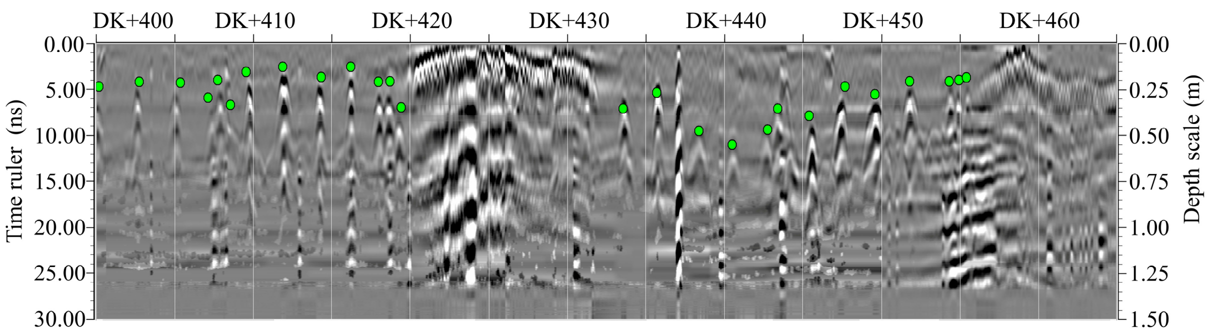

Figure 3. Image of ground-penetrating radar.

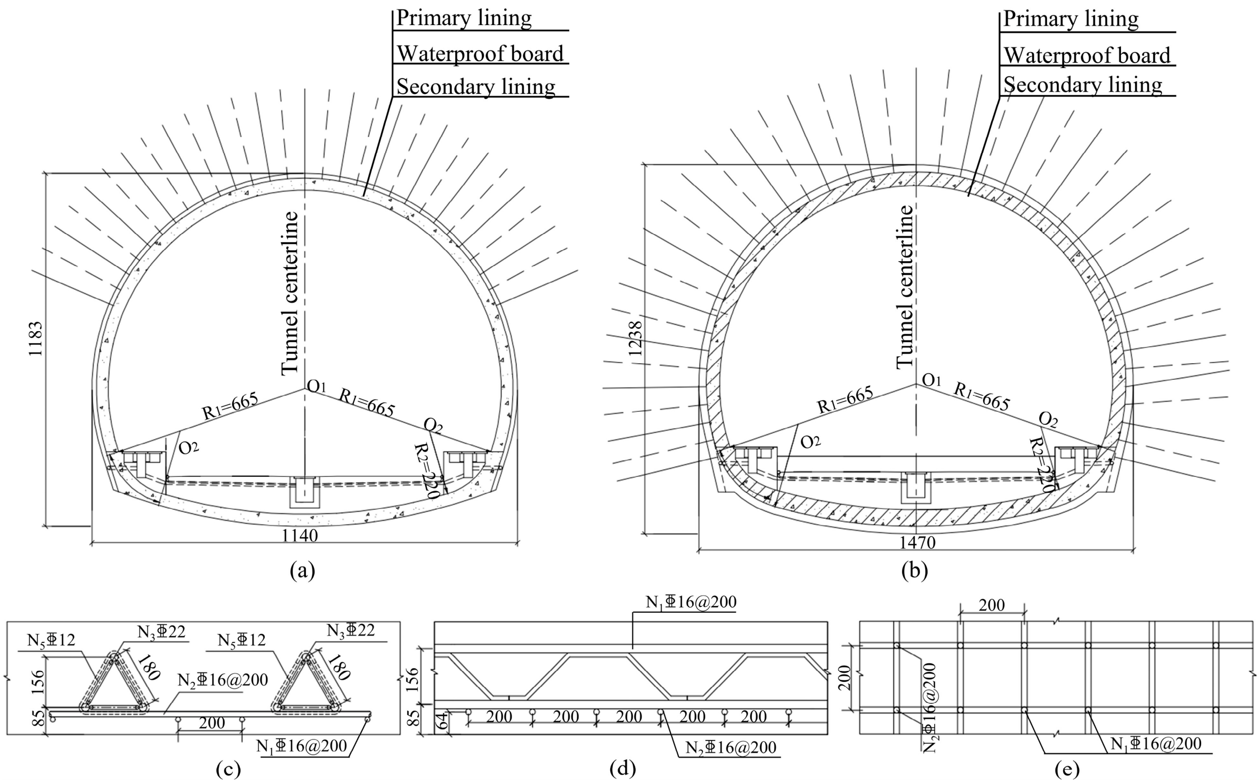

Figure 4. Cross-section design of the studied tunnel at its defective section: (**a**) III_a lining, (**b**) IV_a lining, (**c**) cross-section of the three-leg lattice girders, (**d**) side view of the three-leg lattice girders and (**e**) single-layer anti-crack reinforcement mesh (Unit: mm, except as otherwise stated).

2.2.2. Deformation Characteristics of Defective Section during Construction

The deformation monitoring data for some sections within the tunnel defect section during the construction period are shown in Figure 5. It can be seen from Figure 5 that the vault of section DK265+390 in the defective section settled at 7.2 mm and converged at 6.4 mm, the vault of section DK265+420 settled at 5.4 mm and converged at 7.4 mm, the vault of section DK265+450 settled at 5.4 mm and converged at 9.3 mm and the vault of section DK265+460 settled at 14.5 mm and converged at 8.6 mm. During the construction period, the surrounding rock of the above sections was deformed into the tunnel, the settlement and convergence of the tunnel became stable and the overall deformation was small. This shows that the rock-support system of the defective section reached a stable state during the construction period.

2.2.3. Strength Test of Secondary Lining at Defective Section

The rebound instrument method was used to detect the secondary lining strength of the tunnel defect section. According to the test results, the average value of the C30 concrete strength test in the defective section was 46.3–46.9 MPa and the average value of the C35 concrete strength test was 47.3–51.3 MPa. The Code for Design of Railway Tunnel (TB 10003-2016) [32] requires that the ultimate compressive strength of the C30 concrete for lining not be less than 28.1 MPa, and the ultimate compressive strength of the C35 concrete not be less than 32.5 MPa. Therefore, the strength of the C30 concrete and C35 concrete in the defective section met the design requirements.

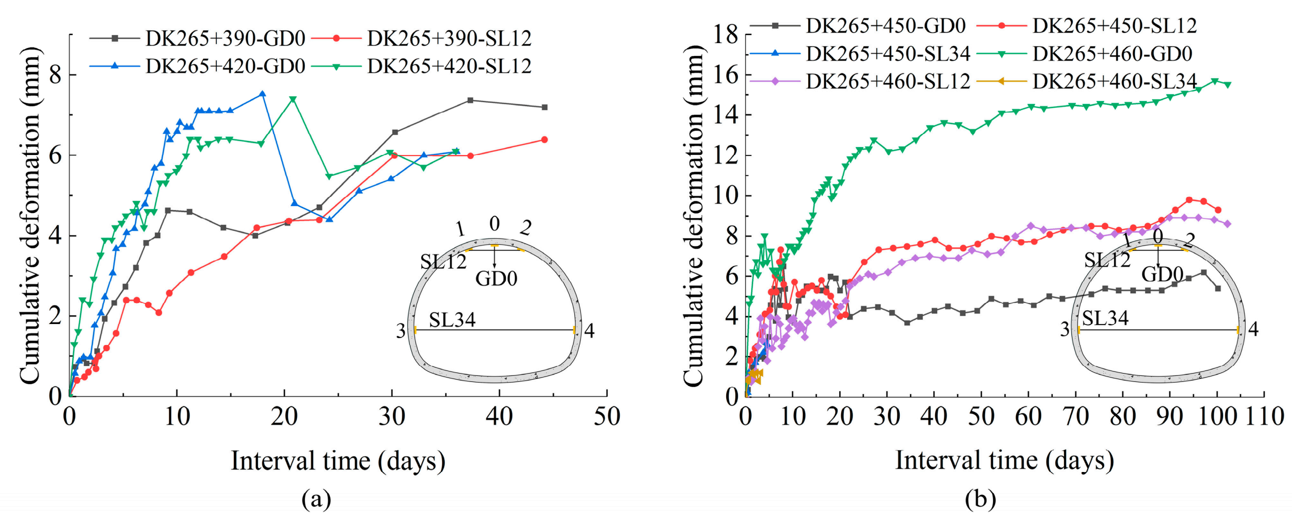

Figure 5. Curve of the accumulated deformation with time during construction of the defective section. (**a**) III_a lining and (**b**) IV_a lining.

3. Safety Evaluation Method

3.1. Load-Structure Method

As the mechanical analysis method for tunnel structure is recommended by the International Tunnelling Association, the load-structure method (bedded-beam model) is widely used in the safety evaluation of tunnel structures [21,33–36]. Based on the plane strain condition, the load-structure method uses springs to simulate the interaction between the lining and surrounding rock. The lining structure is simulated by the beam element and the surrounding rock load is directly applied to the lining structure.

For an analysis of lining safety using the load-structure method, the surrounding rock pressure shall be determined first, then the lining internal force shall be calculated, and finally the safety factor shall be calculated according to the internal force [32,37]. The load-structure method is carried out according to the requirements of Code for Design of Railway Tunnel (TB 10003-2016) [32].

3.1.1. Deep and Shallow Burial Classification

The determination of the deep and shallow burying of the tunnel shall be based on the equivalent height of the load, combined with the geological conditions, construction methods and other factors, according to Equation (1).

$$H_p = (2 - 2.5) \times 0.45 \times 2^{s-1}\omega \tag{1}$$

where H_p is the boundary depth of the shallow tunnel (m) and ω is the width influence coefficient, $\omega = 1 + i(B - 5)$.

Under the conditions of mining method construction, the value of $H_p = 0.9 \times 2^{s-1}\omega$ is taken for Grade IV–VI surrounding rock and the value of $H_p = 1.125 \times 2^{s-1}\omega$ is taken for Grade I–III surrounding rock.

3.1.2. Calculation of Surrounding Rock Pressure under Deep Burial Conditions

The vertical surrounding rock load on the lining of the deep tunnel can be calculated according to Equation (2), and the horizontal uniform pressure can be determined according to Table 1.

$$q = \gamma \times 0.45 \times 2^{s-1}\omega \tag{2}$$

where q is the vertical uniformly distributed pressure (kN/m^2); γ is the unit weight of the surrounding rock (kN/m^3c); s is the grade of the surrounding rock and there is a linear relationship between the grade of surrounding rock and the BQ value [38]; ω is the width influence coefficient, $\omega = 1 + i(B - 5)$; B is the maximum excavation span of the tunnel and the influence of the overbreak shall be considered (m); i is the increase and decrease rate of the surrounding rock pressure for each 1 m increase or decrease of B, based on the vertical uniform pressure of the tunnel surrounding rock with $B = 5$ m, $i = 0.2$ when $B < 5$ m and $i = 0.1$ when $B > 5$ m.

Table 1. Horizontal uniform pressure of surrounding rock.

Surrounding Rock Grade	I–II	III	IV	V	VI
Horizontal Uniform Pressure	0	<0.15 q	(0.15~0.3) q	(0.3~0.5) q	(0.5~1.0) q

3.1.3. Calculation of Surrounding Rock Pressure under Shallow Burial Conditions

Shallow buried tunnels with a basic ground level are loaded symmetrically. The vertical uniform pressure can be determined according to Equations (3)–(5) and the horizontal uniform pressure can be calculated according to Equation (6).

$$q = \gamma H \left(1 - \frac{\delta H \tan\theta}{B}\right) \tag{3}$$

$$\delta = \frac{\tan\beta - \tan\alpha}{\tan\beta[1 + \tan\beta(\tan\varphi_c - \tan\theta) + \tan\varphi_c \tan\theta]} \tag{4}$$

$$\tan\beta = \tan\varphi_c + \sqrt{\frac{\left(\tan^2\varphi_c + 1\right)\tan\varphi_c}{\tan\varphi_c - \tan\theta}} \tag{5}$$

where B represents the tunnel excavation width, m; γ represents the volume weight of the surrounding rock overlying the tunnel, $\mathrm{kN/m^3}$; H represents the buried depth of the tunnel, i.e., the vertical distance from the tunnel arch to the ground, m; θ represents the friction angle of the fracture surface on both sides of the roof soil column; $0.9\varphi_c$ is taken for Class I, II and III surrounding rock, (0.7–0.9) φ_c for Class IV surrounding rock, (0.5–0.7) φ_c for Class V surrounding rock and (0.3–0.5) φ_c for Grade VI surrounding rock, where φ_c is the calculated friction angle of the surrounding rock; δ is the lateral pressure coefficient; β indicates the rupture angle when the maximum thrust is generated.

$$e_i = \gamma h_i \tag{6}$$

where h_i *is* the distance from any point on the inside or outside to the ground, m.

When the load-structure method is used for calculation, the load release caused by the tunnel excavation and the distribution of surrounding rock pressure between the primary support and the secondary lining shall be considered. According to the Technical Manual for Railway Engineering Design (Tunnel Section) [39] and the stratum conditions of the tunnel in this study, the load of the Class III surrounding rock assumed by the secondary lining is 30% of the calculated load, and that of the Class IV surrounding rock is 50% of the calculated load. The distribution of the main loads under deep burial conditions is shown in Figure 6a and the distribution of the main loads under shallow burial conditions is shown in Figure 6b.

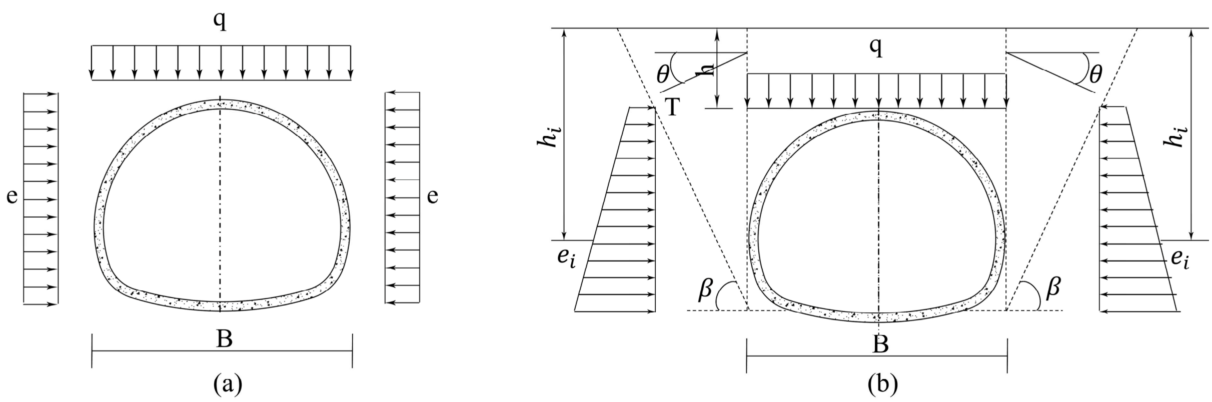

Figure 6. Schematic diagram of surrounding rock load. (**a**) Deep burial condition and (**b**) shallow burial condition.

3.1.4. Safety Factor Calculation and Safety Criteria

To evaluate the safety of the tunnel lining, first analyze the bending moment and axial force of the lining structure. Next calculate the safety factor according to reference to the code [32] and then finally evaluate the safety of the lining structure.

According to the code [32], the concrete lining structure is considered as a compression and bending member in the secondary lining safety evaluation, and the compression safety factor is calculated according to Equation (7).

$$K = \frac{\varphi \alpha R_a bh}{N} \tag{7}$$

where K is the compressive safety factor of the concrete; R_a is the ultimate compressive strength of the concrete; N is the calculated axial force of the concrete section; b represents the section width of the concrete, taking a unit length of 1 m; h is the section thickness of the concrete; φ indicates the longitudinal bending coefficient of the component, which can be taken as 1.0 [32]; α represents the eccentric influence coefficient of the axial force, which is taken according to the specifications [32].

From the crack resistance requirements, the tensile safety factor of a rectangular concrete section with eccentric compression members is calculated according to Equation (8).

$$K = \frac{1.75 \varphi R_l bh}{N\left(\frac{6e_0}{h} - 1\right)} \tag{8}$$

where R_l is the ultimate tensile strength of the concrete and e_0 represents the section eccentricity. The other symbols have the same meaning as in Equation (7).

According to the code [32], when the main load and additional load combination are adopted, if the lining structure of the concrete reaches the compressive limit strength (i.e., the concrete compressive strength control), the safety factor should be ≥2.0; if the lining structure of the concrete reaches the ultimate tensile strength (namely, the concrete tensile strength control), the safety factor should be ≥3.0.

3.2. Short-Term Safety Evaluation

In the early stages of the construction of a high-speed railway tunnel, the deterioration effect of the surrounding rock and concrete will not be considered in the short term; the mechanical properties of the surrounding rock and lining materials are considered to remain basically unchanged. Against the background of this tunnel project, the negative pressure generated by the aerodynamic effects of a high-speed train is the main source of the additional load on the lining structure, and is an important factor affecting the short-term safety of the tunnel. According to the requirements of the code [32], the positive peak pressure generated by the aerodynamic effect is 5.9 kPa and the negative peak pressure is −8.9 kPa. Considering that the positive peak pressure direction is opposite to that of the surrounding rock load, it is equivalent to reducing the surrounding rock load on the loaded lining structure. Therefore, in this study, the negative peak pressure is adopted for the safety evaluation based on the most unfavorable conditions.

3.3. Long-Term Safety Evaluation

According to the requirements of the code [32], the tunnel design needs to ensure 100 years of safe operation. During this period of operation, the repeated influence of positive and negative pressure caused by aerodynamic effects will lead to fatigue damage of the concrete structures. According to the Code for Design of Concrete Structures (GB 50010-2010) [40], when the concrete is subjected to fatigue, the tensile and compressive strength and the elastic modulus of the concrete should be considered for correction. At the same time, the surrounding rock and concrete structure will gradually deteriorate under the effects of the geological environment. Therefore, for the long-term safety evaluation of tunnels, the impact of the comprehensive deterioration of the surrounding rock and concrete, the negative pressure caused by aerodynamic effects and concrete fatigue damage caused by aerodynamic effects should be considered.

According to reference [17], the elastic modulus loss of the surrounding rock is about 40% due to the long-term deterioration effect. According to the Code for Design of Concrete Structures (GB 50010-2010) [40], when concrete is subjected to tension–compression fatigue stress, the correction factor of the compressive strength is 0.6, and the correction factors of C30's and C35's elastic moduli are 0.43 and 0.44, respectively. The long-term elastic modulus and strength of the concrete can be calculated by the following Equations [17].

$$E_c(t) = \frac{X_0 - k_m a\sqrt{t}}{X_0} E_{c0} \tag{9}$$

$$f_c(t) = \frac{X_0 - k_r a\sqrt{t}}{X_0} f_{c0} \tag{10}$$

where E_{c0} is the initial elastic modulus of the concrete, $E_c(t)$ is the elastic modulus of the deteriorated concrete, X_0 is the section height of the lining structure , f_{c0} is the initial compressive strength of the concrete, $f_c(t)$ is the compressive strength of the concrete after deterioration, t is service time, k_m is 0.66, k_r is 0.76 and a = 5.2 × 10^{-4} $(\mathrm{m/day}^{-2})$.

4. Numerical Simulation

4.1. Calculation Condition

A trial calculation for the defective section of the secondary lining structure of the tunnel's DK265+402-420, DK265+432-450 and DK265+450-456 reinforcement mesh was carried out. The results show that the secondary lining of the DK265+402-420 and DK265+432-450 sections can meet the long-term safe operation of the tunnel, while the safety of the DK265+450-456 section is insufficient. Therefore, the most unfavorable situation is taken for discussion in this paper. The calculated defect mileage is DK265+450-456. The surrounding rock class is IV and the buried depth is 29.0 m. According to the geological survey and design data, the surrounding rock is at a relatively good level of grade IV. The lining type is $\mathrm{IV_a}$ and the concrete is C35. According to Equation (1), this mileage section is a deep-buried tunnel. Considering that the defective section is affected by three factors, namely, the deterioration of the surrounding rock and concrete, the negative pressure generated by aerodynamic effects and the concrete fatigue effect caused by aerodynamic effects, a total of five different conditions are set as the numerical simulations for analysis, as shown in Table 2. Among them, condition 1 and condition 2 are for a short-term safety evaluation and condition 3–5 are for a long-term safety evaluation.

Table 2. Numerical simulation conditions.

Condition Name	Description
1	Control group
2	Singular aerodynamic effect
3	Combination of surrounding rock and concrete deterioration
4	Combination of deterioration of surrounding rock and concrete, aerodynamic effects
5	Combination of surrounding rock and concrete deterioration, aerodynamic effects, concrete fatigue effect

4.2. Calculation Parameters

According to the Code for Design of Railway Tunnels (TB 10003-2016) [32], Code for Design of Concrete Structures (GB 50010-2010) [40], geological survey data and on-site strength testing results (Section 2.2.3), the physical and mechanical parameters of the surrounding rock and lining in their current state (before deterioration) must be determined. The elastic reaction coefficient in the current state is 500 MPa/m. The strength parameters of the surrounding rock and concrete after deterioration are determined according to the method in Section 3.3. According to Section 3.3, the elastic modulus after the long-term deterioration of the surrounding rock is set to be 60% of the initial elastic modulus. According to the literature [34], the reaction coefficient of the surrounding rock is proportional to the elastic modulus; the elastic reaction coefficient, considering long-term deterioration, is calculated to be 300 MPa/m. The strength parameters of the surrounding rock and secondary lining are shown in Table 3. Based on the Code for Design of Railway Tunnels (TB 10003-2016) [32], the surrounding rock load values under different working conditions are calculated according to Equation (2) in Section 3.1, as shown in Table 4.

Table 3. Physical and mechanical parameters.

Materials	Gravity (kN/m^3)	Elastic Reaction Coefficient (MPa/m)	Elastic Modulus (GPa)	Poisson's Ratio ν	Compressive Strength (MPa)
Surrounding rock	21.5	500	3.65	0.325	-
Surrounding rock (after deterioration)	21.5	300	2.19	0.325	-
Secondary lining	23.0	-	32.5	0.2	47.3
Secondary lining (after deterioration)	23.0	-	27.1	0.2	38.3
Secondary lining (deterioration + fatigue)	23.0	-	12.04	0.2	23.0

Table 4. Surrounding rock load.

Condition Name	Vertical Load q (kPa)	Horizontal Load e (kPa)
1, 2	75.852	18.963
3, 4, 5	120.435	30.109

4.3. Model Establishment

The safety evaluation analysis of the secondary lining structure of the tunnel used the ANSYS finite element software. The beam element, Beam3, was used to simulate the lining structure and the spring element, Link10, was used to simulate the interaction between the surrounding rock and lining. All the springs only bore a compression load. If the spring was in tension, its force was set to 0. A fixed constraint was applied to the outside of the spring element. The rock loads were applied to the beam elements. The negative pressure load generated by aerodynamic effects was simulated by applying a uniformly distributed load on the lining. When applying the tunnel loads, first, based on the lining elements of the numerical model, the equivalent nodal force was calculated using the ANSYS Parametric Design Language programming Equations (11) and (12) [41,42] and applied to the nodes of the lining elements. The numerical modeling is shown in Figure 7. It should be noted that, for the rationality and accuracy of using the load-structure numerical model for the safety evaluation of the tunnel in this paper, the numerical model and numerical method were validated using on-site experiments of a double-track railway tunnel. The specific verification process can be found in the literature [33].

$$F_i = \begin{bmatrix} F_{xi} \\ F_{yi} \\ M_i \end{bmatrix} = \begin{bmatrix} \frac{7e_1 + 3e_2}{20}|y_j - y_i| \\ -\frac{7q_1 + 3q_2}{20}|x_j - x_i| \\ \frac{1}{60}(y_j - y_i)^2(3e_1 + 2e_2) - \frac{1}{60}(x_j - x_i)^2(3q_1 + 2q_2) \end{bmatrix} \tag{11}$$

$$F_j = \begin{bmatrix} F_{xj} \\ F_{yj} \\ M_j \end{bmatrix} = \begin{bmatrix} \frac{3e_1 + 7e_2}{20}|y_j - y_i| \\ -\frac{3q_1 + 7q_2}{20}|x_j - x_i| \\ -\frac{1}{60}(y_j - y_i)^2(2e_1 + 3e_2) + \frac{1}{60}(x_j - x_i)^2(2q_1 + 3q_2) \end{bmatrix} \tag{12}$$

where F_i and F_j are the equivalent nodal forces of nodes i and j, F_{xi} and F_{xj} are the forces in the x-direction at points i and j, F_{yi} and F_{yj} are the forces in the y-direction at points i and j, M_i and M_j are the bending moments at points i and j, x_i and x_j are the x-axis coordinates of points i and j, y_i and y_j are the y-axis coordinates of points i and j, q_1 and q_2 are the vertical forces applied to the element and e_1 and e_2 are the horizontal forces applied to the element. Due to the fact that it is a deep-buried tunnel section studied in this paper, it can be seen from Figure 6 that $q_1 = q_2$ and $e_1 = e_2$.

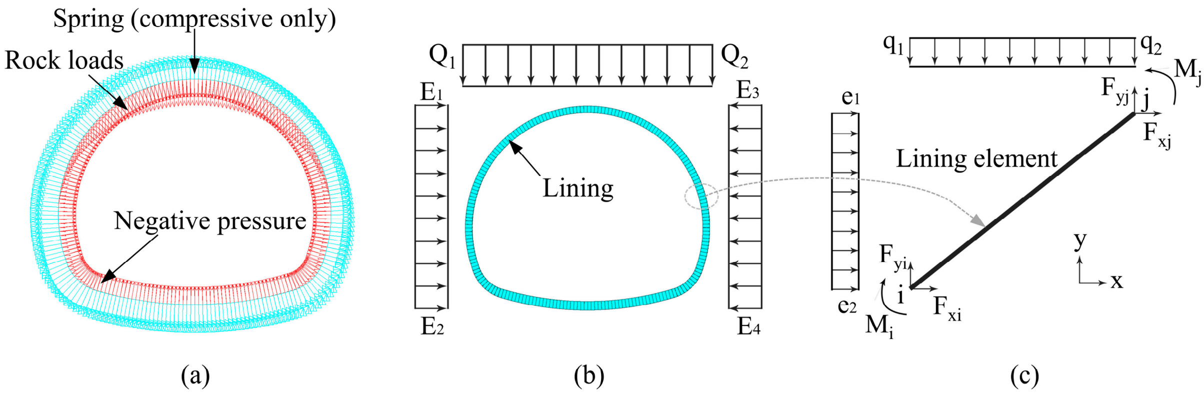

Figure 7. Numerical modeling. (**a**) Applied rock loads and boundary conditions. (**b**) Lining elements and loads distribution. (**c**) Equivalent nodal-force calculation model.

5. Numerical Results and Discussion

5.1. Short-Term Safety Evaluation of Defective Section

Figure 8 shows the diagram of the bending moment and the axial force of the lining in the defective section under condition 1 and condition 2. According to the calculation results of the internal force of the lining in the defective section, the safety factors are calculated as shown in Table 5. It can be seen from the calculation results that the bending moment at the arch crown is the largest under condition 1 and condition 2, which is −66.721 kN·m and −68.862 kN·m, respectively. The axial force at the inverted arch is the highest, which is −785.30 kN and 843.20 kN, respectively. The negative pressure generated by the aerodynamic effects will increase the bending moment and axial force of the lining. When the negative pressure load caused by the aerodynamic effects is considered, the minimum tensile safety factor at the vault increases from 6.274 to 6.514, increasing by 3.8%;

the minimum compressive safety factor at the arch foot is reduced from 21.671 to 19.966, decreasing by 7.9%. The minimum tensile safety factor is 6.274 (greater than 3.0) and the minimum compressive safety factor is 19.966 (greater than 2.0). The safety factors meet the code requirements [32]. The negative pressure generated by the aerodynamic effects has little impact on the short-term safety of the lining in the defective section. The main reason for this is that, under the negative pressure generated by the aerodynamic effects, the lining structure is equivalent to that of adding a uniformly distributed load towards the headroom side of the tunnel, which makes the tensile trend of the lining structure decrease and the compressive trend increase. Therefore, it is not necessary to consider the influence of aerodynamic effects in the short-term safety analysis of similar lining defects.

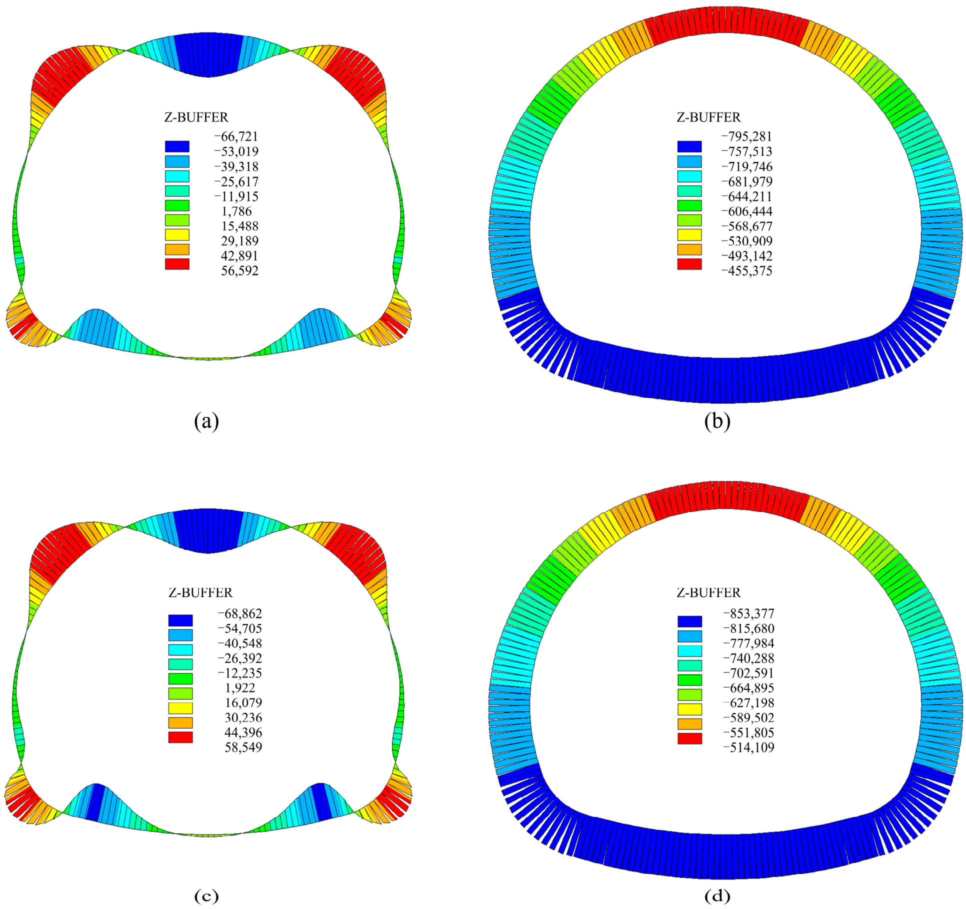

Figure 8. Short-term bending moment and axial force of the defective section. (**a**) Bending moment of condition 1, (**b**) axial force of condition 1, (**c**) bending moment of condition 2 and (**d**) axial force of condition 2.

Table 5. Short-term safety factors of the defective section.

Condition Name	Location	Bending Moment (kN·m)	Axial Force (kN)	e_0/h	Control Status	Safety Factor
1	Vault	−66.721	−473.10	0.353	Tensile control	6.274
	Hance	56.592	−537.90	0.263	Tensile control	10.647
	Arch foot	43.874	−769.93	0.142	Compression control	21.671
	Inverted arch	−52.860	−785.30	0.135	Compression control	27.018
2	Vault	−68.862	−524.63	0.328	Tensile control	6.514
	Hance	58.532	−604.20	0.242	Tensile control	12.094
	Arch foot	47.654	−835.41	0.143	Compression control	19.966
	Inverted arch	−56.536	−843.20	0.134	Compression control	25.190

5.2. Long-Term Safety Evaluation of Defective Section

Figure 9 shows the diagram of the bending moment and axial force of the lining in the defective section under condition 3, condition 4 and condition 5. It can be seen from Figure 9 that the bending moment at the vault is the largest, and the axial force at the inverted arch is the highest. The maximum bending moment and maximum axial force under condition 3 are −108.05 kN·m and 1157.20 kN, respectively, which are 61.9% and 47.4% higher than those under condition 1. The maximum bending moment and maximum axial force of condition 4 and condition 5 have little change when compared to those under condition 3. It can be seen that the deterioration of the surrounding rock and lining materials will lead to a significant increase in the stress on the lining structure. Compared to condition 3, the maximum bending moment and maximum axial force in condition 4 increase by −2.16 kN·m and −54.40 kN, respectively, which is the same as the results in Section 5.1, indicating that the negative pressure load generated by aerodynamic effects will increase the bending moment and axial force of the lining structure. Compared to condition 3, the maximum bending moment in condition 5 decreases by −13.42 kN·m and the maximum axial force increases by −63.7 kN, which is mainly the result of the combined effects of concrete fatigue effect and negative pressure generated by aerodynamics. The fatigue of lining concrete leads to the decrease in strength, modulus, and bearing capacity of the lining. The rock loads are transferred to surrounding rock (i.e., stratum spring). Additionally, the negative pressure generated by aerodynamics will increase the internal force of the lining structure.

It can be seen from Table 6 that the minimum tensile and minimum compressive safety factors in condition 3 are 2.964 and 11.046, which are 52.7% and 49.0% lower than those in condition 1, respectively. The minimum tensile and compressive safety factors in condition 4 are 3.015 and 10.466, which are 51.9% and 51.7% lower than those in condition 1, respectively. Compared to condition 3, condition 4 has a 1.7% increase in the minimum tensile safety factor and a 5.3% decrease in the minimum compressive safety factor. The minimum tensile and compressive safety factors in condition 5 are 3.015 and 10.466, which are reduced by 59.4% and 66.8% when compared to condition 1, and reduced by 14% and 34.9% when compared to condition 3. The safety factors of the vault under condition 3 and condition 5 are less than 3.0, which do not meet the code requirements [32]. The negative pressure generated by a single aerodynamic effect is conducive to reducing the tensile trend of the lining structure. A detailed analysis can be found in Section 5.1. The combined influence of the deterioration of the surrounding rock and support, the negative pressure and concrete fatigue damage will greatly reduce the safety of the lining structure. The adverse effects of the aerodynamic effects on the lining structure are mainly caused by the fatigue damage of the concrete lining and crack development in the lining structure under long-term positive and negative pressure.

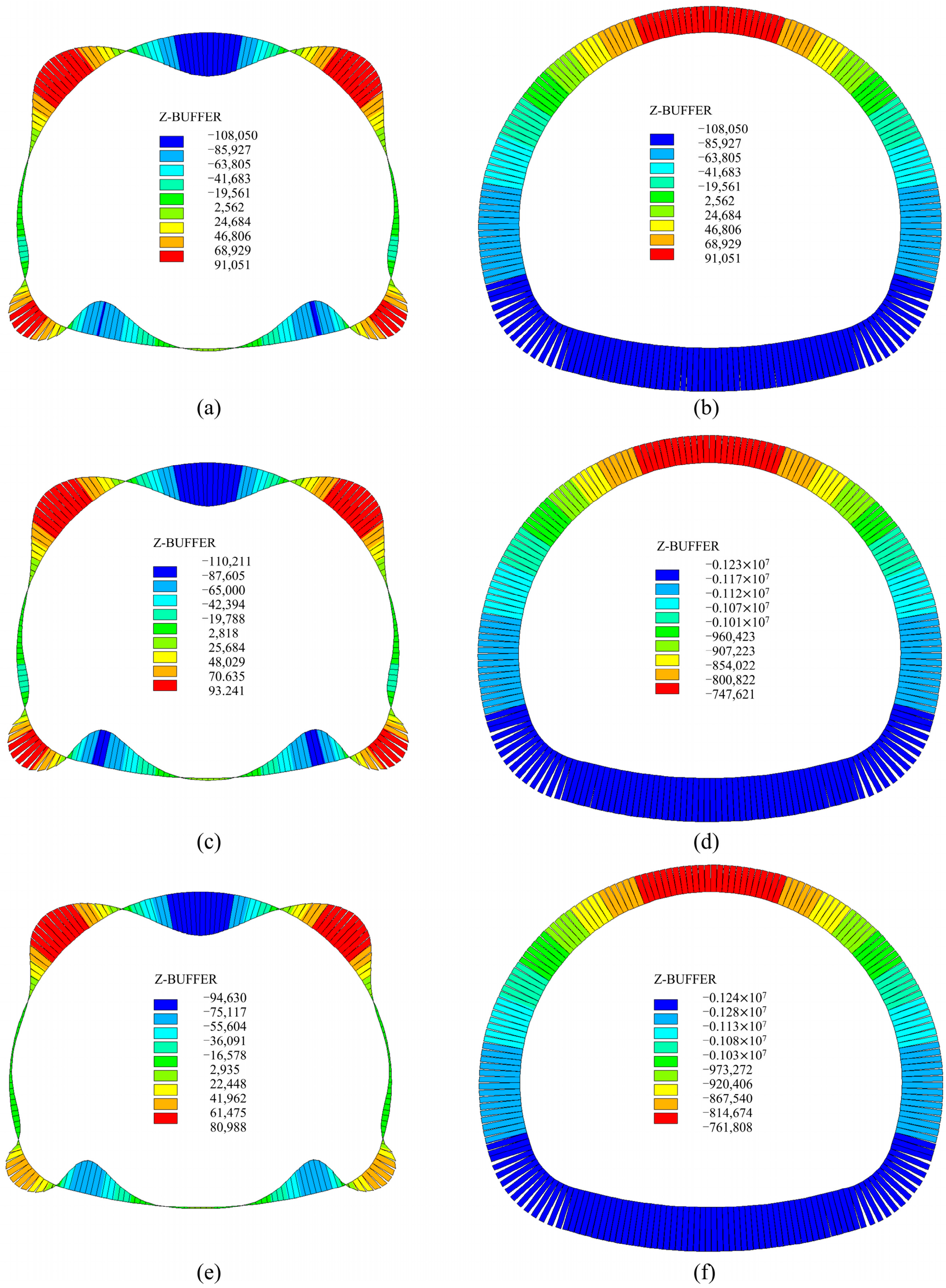

Figure 9. Long-term bending moment and axial force of the defective section. (**a**) Bending moment of condition 3, (**b**) axial diagram of condition 3, (**c**) bending moment of condition 4, (**d**) axial force of condition 4, (**e**) bending moment of condition 5 and (**f**) axial force of condition 5.

Table 6. Long-term safety factors of the defective section.

Condition Name	Location	Bending Moment (kN·m)	Axial Force (kN)	e_0/h	Control Status	Safety Factor
3	Vault	−108.05	−715.94	0.377	Tensile control	2.964
	Hance	90.951	−825.13	0.276	Tensile control	4.974
	Arch foot	77.791	−1139.30	0.171	Compression control	11.046
	Inverted arch	−86.313	−1157.20	0.149	Compression control	14.373
4	Vault	−110.21	−763.68	0.361	Tensile control	3.015
	Hance	93.141	−884.26	0.263	Tensile control	5.229
	Arch foot	82.358	−1199.0	0.172	Compression control	10.466
	Inverted arch	−90.373	−1211.6	0.149	Compression control	13.727
5	Vault	−94.630	−788.50	0.300	Tensile control	2.550
	Hance	80.988	−895.92	0.226	Tensile control	5.046
	Arch foot	51.641	−1207.3	0.107	Compression control	7.193
	Inverted arch	−71.255	−1220.9	0.117	Compression control	8.745

6. Treatment Measures

According to the above research results, it was found that the defective section of the secondary lining will not affect the safe operation of the tunnel in the short-term. However, with an increase in service time, the safety of the vault position is insufficient under the influence of the deterioration of the surrounding rock and concrete. Therefore, in order to ensure the long-term safe operation of the tunnel, strengthening measures should be taken. At present, there are many strengthening measures, but there are also some problems. In 2022, the authors proposed two new strengthening methods for cracked tunnel linings, namely galvanized steel mesh-short bolts (MSB) and galvanized corrugated steel plate-short bolts (PSB) [43], shown in Figure 10. These two strengthening methods have the benefits of fast and convenient construction, have a small impact on lining damage and have good coordination performance after strengthening. The mesh and corrugated plate used in the strengthening method are made from a galvanized steel plate. Galvanized steel has the advantages of low price, good ductility and good durability. The MSB and PSB strengthening methods can transform the brittle failure of the plain concrete lining into a ductile failure, and greatly improve the bearing capacity and toughness of the plain concrete lining structure. After strengthening, the lining structure can continue to bear after cracking, which can effectively prevent the spalling and collapse accidents which occur with plain concrete linings. The detailed experimental results are referred to in the literature [43].

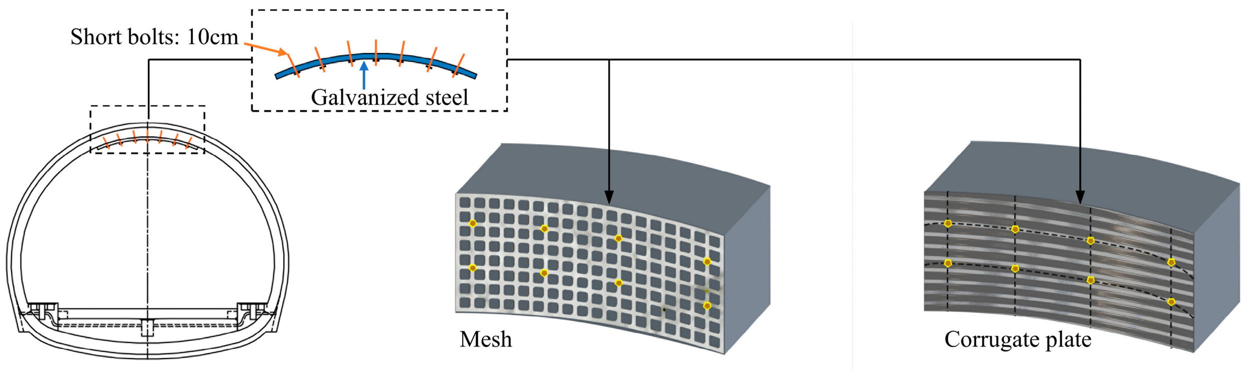

Figure 10. Schematic diagram of MSB and PSB strengthening methods.

It should be noted that when selecting one of these two strengthening methods one should consider whether there is groundwater behind the lining. When there is no underground water behind the lining, there will be no leakage after the lining crack and

MSB can be used for strengthening; otherwise, PSB should be used for strengthening. After strengthening, the lining should be regularly inspected and monitored to ensure the long-term safe operation of the tunnel.

7. Conclusions

Based on engineering principles regarding the anti-crack reinforcement mesh defects of the plain secondary lining used in mountainous high-speed railway tunnels, this paper evaluates the short-term and long-term safety of the defective section of the lining by using a numerical simulation method. Three influencing factors, the deterioration of the surrounding rock and concrete, the negative pressure caused by aerodynamic effects and concrete fatigue damage caused by aerodynamic effects, are considered for a safety evaluation, and corresponding strengthening measures are proposed. The main conclusions are as follows:

(1) The safety of the lining structure can meet the requirements of the code when the defective section of the secondary lining is not affected by other adverse factors. The influence of aerodynamic effects can be ignored in the short-term safety analysis.
(2) When there is deterioration of the surrounding rock and concrete, the safety factor at the vault position of the defective section does not meet the requirements. When considering the combined action of the surrounding rock and concrete deterioration, negative pressure and the concrete fatigue effect, the safety factor of the lining will be further reduced. When evaluating the long-term safety of a plain concrete-lined defect section in a high-speed railway tunnel, the influence of these long-term factors should be considered.
(3) Under the negative pressure caused by the aerodynamic effects, the tensile trend of the lining structure decreases and the compressive stress increases. The influence of the aerodynamic effects on the long-term safety of the tunnel is mainly due to the fatigue damage it causes to the lining of the concrete.
(4) This paper presents a safety evaluation method for anti-crack reinforcement mesh defects in the plain concrete lining of high-speed railway tunnels based on a load-structure method and suggests treatment measures. The research results can provide a reference for future short-term and long-term safety evaluations and treatment of tunnels with quality defects in their plain concrete lining.
(5) This paper only used a numerical simulation to conduct a safety evaluation on the lining of the defective section. In the future, the numerical results should be compared and verified through model tests and on-site monitoring. In addition, further research should be conducted on safety evaluation methods using the ground-structure method to better consider the interaction between the surrounding rock and support.

Author Contributions: Conceptualization, F.L. and J.F.; formal analysis, F.L. and Y.W.; funding acquisition, F.L. and W.Q.; investigation, F.L. and Y.J.; methodology, F.L. and W.Q.; project administration, W.Q.; supervision, W.Q.; validation, F.L. and Y.W.; writing—original draft, F.L., Y.W. and J.F.; writing—review and editing, Y.Y., M.J. and H.L. All authors have read and agreed to the published version of the manuscript.

Funding: This work was supported by Natural Science Foundation of Sichuan Province (No. 2022NSFSC1025), the Natural Science Foundation of China (No. 51991395) and the Talent Introduction Project of Xihua University (No. Z212022).

Institutional Review Board Statement: Not applicable.

Informed Consent Statement: Not applicable.

Data Availability Statement: The data presented in this study are available on request from the corresponding author.

Conflicts of Interest: The authors declare there are no conflict of interest.

References

1. Zhang, Z.; Gong, R.; Zhang, H.; He, W. The Sustainability Performance of Reinforced Concrete Structures in Tunnel Lining Induced by Long-Term Coastal Environment. *Sustainability* **2020**, *12*, 3946. [CrossRef]
2. Wang, F.; Shao, J.; Li, W.; Wang, L.; Wang, Y.; Liu, H. Numerical Simulation Study on Lining Damage of Shield Tunnel under Train Load. *Sustainability* **2022**, *14*, 14018. [CrossRef]
3. Li, H.; Fu, J.; Chen, B.; Zhang, X.; Zhang, Z.; Lang, L. Mechanical Properties of GFRP Bolts and Its Application in Tunnel Face Reinforcement. *Materials* **2023**, *16*, 2193. [CrossRef] [PubMed]
4. Liu, C.; Zhang, D.; Zhang, S. Characteristics and Treatment Measures of Lining Damage: A Case Study on a Mountain Tunnel. *Eng. Fail. Anal.* **2021**, *128*, 105595. [CrossRef]
5. Lu, F.; Wang, H.; Wang, L.; Zhao, K.; Zhang, J. Degradation Law and Service Life Prediction Model of Tunnel Lining Concrete Suffered Combined Effects of Sulfate Attack and Drying–Wetting Cycles. *Materials* **2022**, *15*, 4435. [CrossRef] [PubMed]
6. Fu, J.; Li, H.; Zhu, K.; Chen, Y.; Lei, Z. Study on Expansion Characteristics and Expansion Potential of Gypsum Rock. *Geofluids* **2022**, *2022*, 6921150. [CrossRef]
7. Yu, H.; Zhang, K.; Zhu, X.; Tian, Z.; Zhang, Q. Study on the Freeze-Thaw Process of the Lining Structures of a Tunnel on Qinghai-Tibet Plateau with the Consideration of Lining Frost Damage. *Adv. Mater. Sci. Eng.* **2021**, *2021*, 4921365. [CrossRef]
8. Zhou, B.-Q.; Yang, Z.; Hu, R.; Zhao, X.-J.; Chen, Y.-F. Assessing the Impact of Tunnelling on Karst Groundwater Balance by Using Lumped Parameter Models. *J. Hydrol.* **2021**, *599*, 126375. [CrossRef]
9. Jiang, Y.; Zhang, X.; Taniguchi, T. Quantitative Condition Inspection and Assessment of Tunnel Lining. *Autom. Constr.* **2019**, *102*, 258–269. [CrossRef]
10. Usman, M.; Galler, R. Long-Term Deterioration of Lining in Tunnels. *Int. J. Rock Mech. Min. Sci.* **2013**, *64*, 84–89. [CrossRef]
11. Deng, H.; Fu, H.; Chen, W.; Zhao, Y.; Yi, H. Study on Deterioration, Cracking Mechanism and Treatment Measures of Plain Concrete Lining with Cold Joints in High-Speed Railroad Tunnel. *Case Stud. Constr. Mater.* **2023**, *18*, e01895. [CrossRef]
12. Ye, F.; Qin, N.; Liang, X.; Ouyang, A.; Qin, Z.; Su, E. Analyses of the Defects in Highway Tunnels in China. *Tunn. Undergr. Space Technol.* **2021**, *107*, 103658. [CrossRef]
13. Asakura, T.; Kojima, Y. Tunnel Maintenance in Japan. *Tunn. Undergr. Space Technol.* **2003**, *18*, 161–169. [CrossRef]
14. Zhai, W. *Vehicle–Track Coupled Dynamics*; Springer: Singapore, 2020. [CrossRef]
15. Song, Y.; Wang, Z.; Liu, Z. Study on Aerodynamic Instability and Galloping Response of Rail Overhead Contact Line Based on Wind Tunnel Tests. *IEEE Trans. Veh. Technol.* **2023**. [CrossRef]
16. Song, Y.; Wang, Z.; Liu, Z.; Wang, R. A Spatial Coupling Model to Study Dynamic Performance of Pantograph-Catenary with Vehicle-Track Excitation. *Mech. Syst. Signal Process.* **2021**, *151*, 107336. [CrossRef]
17. Sandrone, F.; Labiouse, V. Analysis of the Evolution of Road Tunnels Equilibrium Conditions with a Convergence–Confinement Approach. *Rock Mech. Rock Eng.* **2010**, *43*, 201–218. [CrossRef]
18. Xu, P.; Wu, Y.; Huang, L.; Zhang, K. Study on the Progressive Deterioration of Tunnel Lining Structures in Cold Regions Experiencing Freeze–Thaw Cycles. *Appl. Sci.* **2021**, *11*, 5903. [CrossRef]
19. Kong, C.; Wang, H.; Zhao, K.; Gao, X. Numerical Simulation of Long-Term Deterioration of Rock Mass Supported by Shotcrete Lining. *Front. Earth Sci.* **2022**, *10*, 891084. [CrossRef]
20. Zhao, Y.; Liu, C.; Zhang, Y.; Yang, J.; Feng, T. Damaging Behavior Investigation of an Operational Tunnel Structure Induced by Cavities around Surrounding Rocks. *Eng. Fail. Anal.* **2019**, *99*, 203–209. [CrossRef]
21. Ye, F.; Han, X.; Qin, N.; Ouyang, A.; Liang, X.; Xu, C. Damage Management and Safety Evaluation for Operating Highway Tunnels: A Case Study of Liupanshan Tunnel. *Struct. Infrastruct. Eng.* **2020**, *16*, 1512–1523. [CrossRef]
22. Lu, P.; Qiao, D.; Wu, C.; Wang, S.; He, X.; Zhang, W.; Zhou, H. Effect of Defects and Remediation Measures on the Internal Forces Caused by a Local Thickness Reduction in the Tunnel Lining. *Undergr. Space* **2022**, *7*, 94–105. [CrossRef]
23. Fu, J.; Xie, J.; Wang, S.; Yang, J.; Yang, F.; Pu, H. Cracking Performance of an Operational Tunnel Lining Due to Local Construction Defects. *Int. J. Geomech.* **2019**, *19*, 04019019. [CrossRef]
24. Han, W.; Jiang, Y.; Li, N.; Koga, D.; Sakaguchi, O.; Chen, H. Safety Evaluation and Failure Behavior of Degraded Tunnel Structure with Compound Diseases of Voids and Lining Defects. *Arab. J. Geosci.* **2021**, *14*, 1531. [CrossRef]
25. Yuan, Y.; Jiang, X.; Ai, Q. Probabilistic Assessment for Concrete Spalling in Tunnel Structures. *ASCE-ASME J. Risk Uncertain. Eng. Syst. Part A Civ. Eng.* **2017**, *3*, 04017011. [CrossRef]
26. Lai, J.; Qiu, J.; Fan, H.; Chen, J.; Hu, Z.; Zhang, Q.; Wang, J. Structural Safety Assessment of Existing Multiarch Tunnel: A Case Study. *Adv. Mater. Sci. Eng.* **2017**, *2017*, 1697041. [CrossRef]
27. Gao, C.; Zhou, Z.; Yang, W.; Lin, C.; Li, L.; Wang, J. Model Test and Numerical Simulation Research of Water Leakage in Operating Tunnels Passing through Intersecting Faults. *Tunn. Undergr. Space Technol.* **2019**, *94*, 103134. [CrossRef]
28. Shi, C.-H.; Wang, A.; Sun, X.-H.; Yang, W.-C. Aerodynamic Behavior and Impact on Driving Safety of Spalling Blocks Comprising High-Speed-Railway Tunnel Lining. *Appl. Sci.* **2022**, *12*, 2593. [CrossRef]
29. Wang, Z.; Ma, W. Dynamic Response and Fatigue-Life Analysis of High-Speed Railway Tunnel Base with Defects. *Math. Probl. Eng.* **2022**, *2022*, 6622998. [CrossRef]
30. Du, J.; Fang, Q.; Wang, G.; Zhang, D.; Chen, T. Fatigue Damage and Residual Life of Secondary Lining of High-Speed Railway Tunnel under Aerodynamic Pressure Wave. *Tunn. Undergr. Space Technol.* **2021**, *111*, 103851. [CrossRef]

31. Li, W.; Liu, T.; Martinez-Vazquez, P.; Chen, Z.; Guo, Z.; Li, M.; Xia, Y.; Liu, H. Aerodynamic Effects of a High-Speed Train Travelling through Adjoining & Separated Tunnels. *Tunn. Undergr. Space Technol.* **2021**, *113*, 103973. [CrossRef]
32. *TB10003-2016*; Code for Design of Railway Tunnel. China Railway Publishing House: Beijing, China, 2016.
33. Zhang, H.J.; Wang, Z.Z.; Lu, F.; Xu, G.Y.; Qiu, W.G. Analysis of the Displacement Increment Induced by Removing Temporary Linings and Corresponding Countermeasures. *Tunn. Undergr. Space Technol.* **2018**, *73*, 236–243. [CrossRef]
34. Papanikolaou, V.K.; Kappos, A.J. Practical Nonlinear Analysis of Unreinforced Concrete Tunnel Linings. *Tunn. Undergr. Space Technol.* **2014**, *40*, 127–140. [CrossRef]
35. Vu, M.N.; Broere, W. Structural Design Model for Tunnels in Soft Soils: From Construction Stages to the Long-Term. *Tunn. Undergr. Space Technol.* **2018**, *78*, 16–26. [CrossRef]
36. Ngan, V.M.; Broere, W.; Bosch, J.W. Structural Analysis for Shallow Tunnels in Soft Soils. *Int. J. Geomech.* **2017**, *17*, 04017038. [CrossRef]
37. *JTG 3370.1-2018*; Design Specification of Highway Tunnel. China Communications Press: Beijing, China, 2018.
38. Wang, M.; Wang, Z.; Tong, J.; Zhang, X.; Dong, Y.; Liu, D. Support Pressure Assessment for Deep Buried Railway Tunnels Using BQ-Index. *J. Cent. South Univ.* **2021**, *28*, 247–263. [CrossRef]
39. Second Design Institute of Ministry of Railways. *Railway Engineering Design Technical Manual—Tunnel*; China Railway Publishing House: Beijing, China, 1999.
40. *GB 50010-2010*; Code for Design of Concrete Structures. China Building Industry Press: Beijing, China, 2015.
41. Showkati, A.; Salari-rad, H.; Hazrati Aghchai, M. Predicting Long-Term Stability of Tunnels Considering Rock Mass Weathering and Deterioration of Primary Support. *Tunn. Undergr. Space Technol.* **2021**, *107*, 103670. [CrossRef]
42. Li, Z.; Zeng, Y. *Principles and Methods of Underground Structure Design*; Southwest Jiaotong University Press: Chengdu, China, 2003.
43. Lu, F.; Li, P.; Zheng, Y.; Chou, W. Experimental Investigation on the Mechanical Performance of Retrofitted Cracked Linings with Mesh-bolts and Plate-bolts. *China J. Highw. Transp.* **2022**, *35*, 128–139. [CrossRef]